Heliyon 9 (2023) e22022

Contents lists available at ScienceDirect

Heliyon

journal homepage: www.cell.com/heliyon

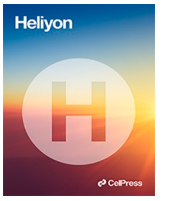

# Hydrothermal dewatering of low-grade coal: Product evaluation and primary component analysis of ash deposition

Datin Fatia Umar *, Zulfahmi Zulfahmi, Triswan Suseno, Suganal Suganal, Nendaryono Madiutomo, Liston Setiawan, Edwin Akhdiat Daranin, Gunawan Gunawan

*Research Centre for Mining Technology, National Research and Innovation Agency, The Republic of Indonesia, Jalan Sutami KM 15, Tanjung Bintang 35361, Lampung, Indonesia*

ARTICLE INFO

*Keywords:*
Low-rank coal
hydrothermal
ash deposition
Paired sample *t*-test
PCA

ABSTRACT

The hydrothermal dewatering (HTD) process was carried out using 16 coal samples obtained from several regions in Indonesia. This research aims to identify the dominant parameters that influence ash deposition during coal combustion in a boiler or gasifier due to the HTD process. This research was conducted due to the lack of clear and comprehensive information regarding this issue. Therefore, to understand the effect of HTD on ash deposition, an analysis of the chemical composition of ash and the ash melting temperature (AFT) was carried out. To verify the data obtained from the experimental analysis, statistical methods such as paired sample *t*-test and primary component analysis were applied to obtain the dominant parameters influencing ash deposition due to HTD. Eight parameters, namely $SiO_2$, $Fe_2O_3$, slagging viscosity index (SR), Babcock index (Rs), initial deformation temperature, softening temperature, hemispherical temperature, and fluid temperature under oxidative conditions, have the greatest influence on ash deposition due to the HTD process. Based on the average values of SR and Rs, raw coal and processed coal samples have the same ash deposition trend. On the other hand, based on AFT under oxidation conditions, processed coal has a higher AFT, indicating that the tendency for ash deposition is lower than raw coal. Therefore, the HTD process can be used to improve the quality of low-grade coal. As an implication, low-grade coal, which has not been widely utilized in Indonesia, due to several constraints regarding its characteristics, through the HTD process can be optimized where coal utilization is a bridge towards the use of green energy which is being intensively pursued.

## 1. Introduction

Currently, Indonesia has 151.399 billion tons of coal resources and 39.89 billion tons of coal reserves, most of which are distributed throughout Sumatra and Kalimantan [1]. The distribution of coal resource quality in Indonesia is categorized as medium-calorie (53.62 %), low-calorie (36.02 %), high-calorie (8.70 %), and very-high-calorie (1.66 %).

The reserves of medium-, low-, high-, and very high-quality are 54.10 %, 38.46 %, 6.32 %, and 1.12 %, respectively. Based on the Indonesian Government Regulation No. 45 of 2003 on Tariffs of Non-Taxable Government Revenue from the Ministry of Energy and

* Corresponding author.
*E-mail address:* dati001@brin.go.id (D.F. Umar).

https://doi.org/10.1016/j.heliyon.2023.e22022
Received 9 May 2023; Received in revised form 1 November 2023; Accepted 2 November 2023
Available online 9 November 2023

Mineral Resources, low-calorie coal has a calorific value (CV) of <5100 kcal/kg, while that of medium-calorie coal is 5100–6100 kcal/kg, that of high-calorie coal is 6100–7100 kcal/kg, and that of very high-calorie coal is > 7100 kcal/kg on an air-dried basis (adb) [2].

Lignite and subbituminous coal are classified as low-grade coals and generally have a low CV, high moisture content (25–65 %), and low sulfur content [3]. High moisture content in coal causes problems during utilization, especially when it is used directly as a fuel. During combustion, moisture reduces the CV of coal; therefore, more coal is required. Moreover, a considerable amount of carbon dioxide ($CO_2$) gas is produced. High levels of $CO_2$ gas negatively impact the environment owing to the emergence of the greenhouse effect, which can lead to global warming [4]. In addition, low-grade coal suffers from the formation of ash deposits, which are usually associated with the low-melting minerals in coal [5]. To increase the utilization of low-grade coal, an upgrading process is required to enhance its properties to resemble those of high-grade coal.

Several coal-upgrading technologies have been developed and utilized to reduce the water content in coal. Evaporation-based drying techniques, such as rotary drying, fluid-bed drying, and hot oil immersion, and drying by non-evaporative techniques, such as hot water drying have been utilized [4]. The main reasons for using these processes are to reduce transportation costs, eliminate handling problems, and increase coal combustion efficiency. Hydrothermal dewatering (HTD) is a typical non-evaporative drying method. Typically, the temperature and pressure ranges of the HTD process are 200–350 °C and 10–25 MPa, respectively [6]. The HTD process significantly reduces the moisture content of low-grade coals and, thus, increases their CV and quality. This process is believed to replicate natural coal formation because of its high pressure and temperature [7]. Research on this technology has mainly focused on the influencing factors, composition of the HTD products, and combustion characteristics [8,9]. After the HTD process, the treated coal had better combustion characteristics than the raw coal, including higher ignition and a lower tendency for spontaneous combustion. From this perspective, the HTD process may improve the quality of low-grade coal to be comparable with that of high-grade coal.

In Indonesia, coal is mainly used as a fuel in coal-fired power plants (CFPPs) to produce electricity. Currently, the contribution of coal to electricity generation is the largest, generating 36.98 GW or 50.14 % of the total electricity generated [10]. In almost all CFPPs, ash deposition by slagging and fouling varies depending on the coal quality and operating conditions [11]. Slagging refers to the deposition occurring in sections of the boiler where radiation-induced heat transfer is dominant, whereas fouling is defined as the formation of deposits on the surface of convective tube bundles. Both processes are very serious because they not only reduce the heat transfer and efficiency of the boiler but also degrade the superheaters, thereby leading to unscheduled shutdowns. Moreover, these processes involve deposition on the heat transfer surfaces, the formation of difficult-to-collect fine particles, and the erosion and corrosion of the surface [12].

The phenomenon of ash deposition is mainly influenced by the chemical composition and fusion behavior of the coal ash. The chemical composition of the ashes was obtained in oxide form from the non-combustible components produced by burning coal. Three groups of oxides were detected: acids ($SiO_2$, $TiO_2$, and $P_2O_5$), amphoteric oxides ($Al_2O_3$ and $Fe_2O_3$), and bases ($Na_2O$, $K_2O$, CaO, MgO, and MnO). Alternatively, by dividing these oxides into two groups, $Al_2O_3$ is assigned to the acidic oxide group and $Fe_2O_3$ to the basic oxide group [13]. The formation of slag is mainly influenced by $Fe_2O_3$, CaO, MgO, $K_2O$, $Na_2O$, $SiO_2$, $Al_2O_3$, and $TiO_2$ [14]. For the prediction of ash deposition by slagging and fouling in boilers, most researchers measure the base-to-acid (B/A) ratio, bed agglomeration index (BAI), fouling index (Fu), slag viscosity index (SR), and Babcock index (RS) of coal [15–17]. Some researchers reported that the HTD process can remove alkali metals, such as potassium, sodium, titanium, iron, calcium, and magnesium, from coal. These metals significantly affect ash deposition during coal combustion [18–20].

The fusion behavior of ash is critical for the selection of coal and the operation of boilers and gasifiers. It is necessary to avoid ash sintering and ensure smooth slagging. The ash fusion behavior can be evaluated using different methods, including the ash fusion temperature (AFT). Four characteristic temperatures were defined based on the shape transformation of the ash cone at elevated temperatures: the initial deformation temperature (IDT), softening temperature (ST), hemispherical temperature (HT), and fluid temperature (FT) [21].

The effect of the HTD process on ash deposition considers only the calculation of several indices based on the chemical composition analysis, and thus the determination of the AFTs is difficult. Therefore, it is necessary to conduct statistical tests to determine the main parameters influencing ash deposition. A paired-sample *t*-test was used to determine whether the mean difference between two data sets was significant [22], and principal component analysis (PCA) was also applied to summarize the information contained in large data tables by utilizing a smaller set of indices that could be visualized and analyzed more easily [23].

Studies on the investigation of the factors affected by the HTD process, which consequently influence the ash composition and ash fusion behavior, are very limited and unclear. These studies were performed using Samarinda (East Kalimantan), Tanjung (South Kalimantan), and Lahat (South Sumatra) coals as internal reports, but these studies were not comprehensive [24]. Therefore, this paper describes the effect of the HTD process on ash deposition during combustion in a boiler or gasifier based on the ash chemical composition and fusion behavior. In this study, the ash deposition of raw lignite and hydrothermally treated coal were investigated. The characteristics of the raw and treated coal samples were evaluated based on the proximate, ultimate, and CV analysis results. Indices based on the ash chemical analysis and AFT were determined to predict the occurrence of ash deposition during combustion in CFPPs or gasification reactors.

## 2. Experimental

### 2.1. Coal sampling

A total of 16 low-grade coal samples were collected from various coal mining areas, including Muara Enim (ME), Tebo Ilir (TB), Bayung Lencir (BL), Gunung Mas (GM), Kutai Barat (KB), Tanjung Palas (TS), Adaro (AD), Kintap (AK), Satui (AR), Bukit Asam (BP),

Berau (BJ), Banjarsari (BS), Papua (PP), Gelubir (GB), Muarabara (MB), and Wahau (WH), located in the Sumatra and Kalimantan Islands of Indonesia. A purposive sampling technique was used, which emphasizes several criteria and characteristics of certain coals according to the research topic [25]. Homogeneous samples were selected because they had the same characteristics as those of the bulk material. The selection of sampling locations was based on previous data, which stated that there are low-grade coal resources in the area that have not been optimally utilized. Using this HTD process, coal is expected to be utilized more optimally in the future.

Coal samples were collected from the surface of the coal stockpiles according to ASTM Standard D 6610–01a: 'Standard Practice for Manually Sampling Coal from the Surfaces of a Stockpile', which provided bulk samples for general laboratory analyses and the estimation of quality and total moisture. This procedure involves manually collecting increments from various locations near the stockpile surface and combining them into one or more bulk samples. Each increment was collected, sealed in plastic-lined canvas bags, and identified. The coal samples were transferred to a coal laboratory for analysis and HTD.

### 2.2. Coal characterization

In the coal laboratory, the raw coal samples were crushed and passed through a ±3-mm sieve for hydrothermal processing and through a 250-μm sieve (no. 60) for the analysis of the proximate, ultimate, and calorific values, including the ash chemical and AFT analyses. The proximate analysis of the samples included the determination of the inherent moisture (IM), ash (A), and volatile matter (VM), according to ASTM D 3176, ASTM D 3175, and ASTM D 3175, respectively. The fixed carbon (FC) content on a dry basis (db) was calculated as 100%–% (A + VM). The ultimate analysis included the determination of the carbon and hydrogen contents according to ASTM D 3179-89, the nitrogen content according to ASTM D 3179, the total sulfur content using the infrared method, and the oxygen content on a dry ash-free (daf) basis calculated at 100 % (C + H + N + S). Based on the results, the H/C and O/C atomic ratios were obtained, which are often used as indicators of the degree of carbonization [26]. The atomic H/C and O/C ratios are high for fuels with a low degree of carbonization, such as peat and lignite. Using the HTD process, it is expected that these ratios will decrease in the same range as that for high-grade coal. In addition, the CV was determined according to ASTM standard 5865-04.

### 2.3. Hydrothermal dewatering process

The HTD process was conducted at a laboratory scale in an autoclave with a batch capacity of 10 L. Approximately 1500 g of pulverized coal with a particle size of less than 3 mm was homogeneously mixed with 3500 g of distilled water. Subsequently, the resulting slurry was placed in an autoclave, which was sealed, evacuated for 5 min to remove trapped air, and filled with $N_2$ at a pressure of approximately 0.1 MPa. The autoclave was heated to 330 °C at a rate of 3–4 °C/min, stirred at 75 rpm, and maintained at this temperature for 30 min under continuous stirring [27]. After the autoclave was cooled to the ambient temperature, the processed coal was removed and washed with distilled water. The coal samples were then filtered, dried, and stored in sealed containers. The HTD-treated coal samples were marked as MET, TBT, BLT, GMT, KBT, TST, ADT, AKT, ART, BPT, BJT, BST, PPT, GBT, MBT, WHT and then analyzed in the same manner as the raw coal samples.

### 2.4. Ash deposition prediction

To conduct the ash deposition prediction, the raw and HTD-treated coal samples were converted to ash at 400 °C for 10 h to prevent the release of alkali metals [27]. The ash composition analysis of $SiO_2$ was determined by gravimetry, $TiO_2$ and $P_2O_5$ by spectrophotometry, $SO_3$ by turbidimetry, and $Al_2O_3$, $Fe_2O_3$, CaO, MgO, $Na_2O$, $K_2O$, and $MnO_2$ by atomic absorption spectrometry (AAS) [28].

The various empirical indicators of depositional tendencies based on ash composition, such as B/A, BAI, Fu, SR, and Rs in the mass percent ratio, including several indices that are used for PCA, such as the ratio of silica to calcium and magnesium (Si/Ca + Mg), the ratio of silica, phosphor, and potassium to calcium and magnesium (Si + P + K)/(Ca + Mg), the silica/potassium (Si/K) ratio, the aluminum content divided by 200 (Al/200), the iron/manganese (Fe/Mn) ratio, and the ratio of the base to the acid including phosphorous (B/A + P) were determined according to Eqs (1)–(11) [5,23,29,30].

$$\frac{B}{A}=\frac{(Fe_2O_3+CaO+MgO+Na_2O+K_2O)}{(SiO_2+Al_2O_3+TiO_2)} \tag{1}$$

$$BAI=\frac{Fe_2O_3}{Na_2O+K_2O} \tag{2}$$

$$Fu=\frac{B}{A}x(Na_2O+K_2O) \tag{3}$$

$$SR=\frac{SiO_2\times 100}{SiO_2+Fe_2O_3+CaO+MgO} \tag{4}$$

$$Rs=\frac{B}{A}\times(S) \tag{5}$$

$$\frac{Si}{Ca+Mg}=\frac{SiO_2}{CaO+MgO} \tag{6}$$

$$\frac{Si+P+K}{Ca+Mg}=\frac{SiO_2+P_2O_5+K_2O}{CaO+MgO} \tag{7}$$

$$\frac{Si}{K}=\frac{SiO_2}{K_2O} \tag{8}$$

$$\frac{Al}{200}=\frac{Al_2O_3}{200} \tag{9}$$

$$\frac{Fe}{Mn}=\frac{Fe_2O_3}{MnO} \tag{10}$$

$$\frac{B}{A}+P=\frac{(Fe_2O_3+CaO+MgO+Na_2O+K_2O)}{(SiO_2+Al_2O_3+TiO_2)}+P_2O_5 \tag{11}$$

Slagging hazards depend on the properties of the ash [5]. Generally, the slagging tendency increases with the B/A ratio. An ash sample has a low slagging tendency when the B/A ratio is $< 0.5$, a medium slagging tendency for B/A ratios between 0.5 and 0.99, a high slagging tendency for B/A ratios between 1 and 1.74, and a severe slagging tendency for B/A $> 1.75$ [29].

The BAI was expanded to evaluate the problems during fluidized bed combustion operations. Bed agglomeration occurs when the BAI is $< 10$ [31]. The fouling index of Fu [32] is based on the B/A ratio but also considers the alkali ($Na_2O + K_2O$) content. Higher Fu values correspond to higher fouling tendencies [33]. A low fouling tendency is expected for Fu $< 0.6$, a medium fouling tendency occurs for Fu between 0.6 and 40, and a high fouling tendency occurs for Fu $> 40$.

A high SR index indicates a high slag viscosity and thus low slagging. When SR $> 72$, the tendency to form impurities is low. When the SR index ranges between 65 and 72, the tendency to form impurities is average. When the SR index is $< 65$, the tendency to form impurities is very high [20]. The prediction of the slagging/Babcock index (Rs) at the furnace wall during boiler operation is based on the B/A ratio of the coal ash and the percentage of sulfur in the sample on a dry basis. Higher Rs values indicate a higher propensity for slagging [29]. A low slagging tendency occurs for Rs $< 0.3$, a medium slagging tendency occurs for Rs values between 0.6 and 2.0, a high slagging tendency for Rs values between 2.0 and 2.6, and a severe slagging tendency for Rs $> 2.6$.

In addition to the chemical composition of the ash, the temperature range derived from the AFT can be used to assess the slagging potential of the fuel [34]. AFT analysis was performed according to ASTM D1857-04 2013 to determine the fusibility of the raw and treated coal samples in either reductive or oxidative conditions. During the test, in the reductive conditions, a mixture of $CO_2$ (40 %) and CO (60 %) gases was supplied, while in the oxidative condition, a mixture of $CO_2$ (50 %) and $O_2$ (50 %) gases was supplied [35]. The ash, in the form of a pyramid, was gradually heated to 1000–1550 °C under both reductive and oxidative conditions, and the AFTs were monitored as follows [36].

- Initial deformation temperature (IDT): The temperature at which ash begins to flow.
- Softening temperature (ST): The temperature at which ash softens and becomes plastic.
- Hemispherical temperature (HT): The temperature at which a hemispherically shaped droplet forms.
- Fluid temperature (FT): The temperature at which ash becomes a free-flowing fluid.

The paired-sample *t*-test and PCA were used to determine the dominant factors influencing ash deposition. The paired-sample *t*-test was used to compare the difference between the two population means in the matched sample design. This test assumes that the observations are typically distributed and uncontaminated. Tests used to compare the means of two groups are usually restricted by the assumptions of normality and homogeneity of variances [37]. This test was applied to obtain the most influential variable for coal ash deposition by comparing two paired data samples measured twice, before and after the HTD process.

PCA derives dimensions by combining variables into a small number of principal components [38]. The measured objects were variables that affected ash deposition either in the boiler during combustion or gasification in the power plant. In total, there were 36 components, including the ash and sulfur contents, chemical ash composition, AFTs before and after the HTD process, and indices of ash deposition based on the chemical ash composition. PCA was constructed such that each component describes as much of the variation in the data as possible. The components were ranked in decreasing order of explained variance, and were all uncorrelated. Data were processed using the Statistical Package for Social Science (SPSS) software.

## 3. Results and discussion

### 3.1. Effect of the HTD process on the chemical properties of coal

HTD is a non-evaporative process that effectively removes water and changes the chemical structure of lignite [9]. The calorific, proximate, and ultimate values of the raw and treated coals are listed in Table 1. The IM of all the raw coal samples is relatively high (>10 %), ranging from 10.1 % to 36.38 % on an adb. Notably, coal with high IM has a relatively low CV. These results were consistent

with those of Liao et al. [9]. Raw coal has a lower CV, resulting in a lower combustion efficiency in CFPPs. Therefore, $CO_2$ emissions are also higher.

After HTD, the IM decreased significantly. Therefore, the HTD process was confirmed to be effective in reducing the moisture content of coal, until a normal equilibrium is reached relative to the moisture content of the surrounding air. Generally, the ash content of the treated coal samples increased slightly, whereas the VM decreased and the FC increased.

The reduction in the IM and VM in the treated coals after the HTD process causes the FC to increase. A higher FC content facilitates effective coal combustion [39]. Therefore, the FC/VM fuel ratio also increased. Lower fuel ratios lead to high ignition behavior and may cause the spontaneous ignition of coal during stockpiling. Higher fuel ratios cause difficulty in coal ignition but result in a stable combustion process [40].

Ignitability, defined as coal's flammability, significantly impacts the flame stability and pollutant formation processes in CFPPs [41]. Moreover, the ignition characteristics of coal play an important role in boiler design and combustion optimization. The ignitability index (Ii) is an effective indicator of coal ignition. This indicates the likely performance of a given coal under furnace conditions. The Ii was calculated based on Eq. (12) [42,43].

$$Ii = \frac{(CV - 81FC)}{(VM + IM)} \tag{12}$$

where FC, VM, and IM (weight percentage, wt%), and CV (kcal/kg) were all on an adb. Table 2 indicates that the treated coal samples had higher values for both the ignitability index (Ii) and the fuel ratio compared to the raw coal samples. The increase in Ii is due to the higher calorific value and the lower VM and IM values. The increase in fuel ratio is due to the higher FC value and the lower VM value. If a solid fuel has an Ii of $<35$, it may be difficult for the boiler to efficiently utilize the fuel [42]. Almost all the raw coal samples, except AD, AR, and BS, had an Ii of $<35$. However, after HTD treatment, the Ii of all the treated coal samples increased significantly to $>50$.

The ultimate analysis results revealed that after the HTD process, the carbon content increased, and the oxygen content decreased significantly (Table 2). As shown in the Van Krevelen diagram (Fig. 1), the reduction in the atomic ratios of O/C and H/C, two parameters related to the coal grade, indicates the removal of oxygen-containing functional groups and improvements in the coal grade [26].

The O/C and H/C ratios of the raw and treated coal samples in the van Krevelen coal band decreased from lignite to low- or medium-grade bituminous coal, although they did not proceed exactly along the coal band. The data suggest that the HTD process can upgrade low-grade coal to a level comparable to that of bituminous coal, particularly in terms of carbon content. HTD can be

**Table 1**
Calorific value, proximate, and ultimate analyses of the raw and treated coals.

| | CV cal/g db | IM % adb | Ash % db | VM % db | FC % db | C % daf | H % daf | N % daf | S% % daf | O % daf |
|---|---|---|---|---|---|---|---|---|---|---|
| ME | 5464 | 12.97 | 6.46 | 51.91 | 41.63 | 69.65 | 6.51 | 0.75 | 0.25 | 22.84 |
| MET | 6487 | 2.84 | 8.43 | 43.56 | 48.01 | 82.30 | 5.75 | 1.05 | 0.19 | 10.72 |
| TB | 5426 | 10.78 | 6.60 | 49.18 | 44.22 | 70.29 | 6.17 | 0.95 | 0.66 | 21.94 |
| TBT | 6518 | 4.18 | 7.10 | 40.37 | 52.54 | 80.40 | 5.41 | 1.26 | 0.61 | 12.32 |
| BL | 6587 | 30.85 | 4.01 | 52.96 | 43.04 | 73.55 | 11.19 | 1.93 | 3.05 | 10.28 |
| BLT | 7471 | 3.75 | 4.89 | 46.65 | 48.46 | 81.48 | 6.37 | 1.44 | 3.22 | 7.48 |
| GM | 5936 | 20.87 | 3.12 | 49.50 | 47.38 | 73.22 | 7.58 | 0.87 | 0.14 | 18.19 |
| GMT | 6772 | 3.46 | 4.86 | 44.99 | 50.16 | 80.99 | 5.12 | 1.07 | 0.19 | 12.64 |
| KB | 6416 | 19.94 | 1.40 | 51.20 | 47.40 | 73.17 | 8.17 | 0.77 | 0.19 | 17.70 |
| KBT | 7149 | 4.57 | 2.31 | 43.45 | 54.25 | 81.60 | 6.05 | 1.39 | 0.21 | 10.74 |
| TS | 6097 | 35.35 | 1.59 | 53.07 | 45.34 | 72.67 | 11.00 | 0.85 | 0.71 | 14.77 |
| TST | 7074 | 4.3 | 2.72 | 40.74 | 56.54 | 67.50 | 5.80 | 1.00 | 0.60 | 25.11 |
| AD | 6383 | 10.33 | 3.16 | 52.64 | 44.21 | 71.33 | 6.08 | 0.73 | 0.11 | 21.76 |
| ADT | 7224 | 2.73 | 5.35 | 47.77 | 46.88 | 81.36 | 5.43 | 0.96 | 0.17 | 12.08 |
| AK | 6424 | 27.85 | 4.09 | 51.25 | 44.66 | 70.61 | 8.67 | 0.82 | 0.18 | 19.72 |
| AKT | 7018 | 10.86 | 6.25 | 41.77 | 51.99 | 82.64 | 6.25 | 1.17 | 0.22 | 9.72 |
| AR | 6879 | 10.1 | 1.42 | 50.76 | 47.82 | 73.81 | 6.19 | 0.81 | 0.20 | 18.98 |
| ART | 7599 | 3.99 | 3.16 | 43.17 | 53.67 | 82.14 | 5.56 | 1.01 | 0.11 | 11.18 |
| BP | 6145 | 23.63 | 3.16 | 53.11 | 43.73 | 71.53 | 8.17 | 0.70 | 0.14 | 19.46 |
| BPT | 6980 | 4.96 | 5.88 | 41.45 | 52.67 | 81.91 | 5.43 | 0.96 | 0.22 | 11.47 |
| BJ | 5960 | 17.73 | 4.98 | 54.09 | 40.93 | 68.94 | 7.09 | 0.88 | 0.39 | 22.70 |
| BJT | 6965 | 4.01 | 8.50 | 38.41 | 53.09 | 80.88 | 5.33 | 1.21 | 0.36 | 12.22 |
| BS | 6329 | 16.77 | 7.50 | 49.06 | 43.45 | 72.45 | 7.09 | 0.97 | 2.13 | 17.36 |
| BST | 7129 | 3.78 | 7.84 | 40.97 | 51.20 | 81.15 | 5.46 | 1.20 | 1.91 | 10.29 |
| PP | 5562 | 26.76 | 9.48 | 52.68 | 37.85 | 68.85 | 8.76 | 1.13 | 2.02 | 19.23 |
| PPT | 6611 | 2.34 | 11.51 | 41.46 | 47.03 | 80.90 | 5.52 | 1.45 | 1.81 | 10.33 |
| GB | 5019 | 18.83 | 16.63 | 48.08 | 35.28 | 70.25 | 6.69 | 0.46 | 0.16 | 22.43 |
| GBT | 5942 | 4.04 | 19.01 | 42.67 | 38.32 | 81.83 | 5.35 | 0.98 | 0.08 | 11.75 |
| MB | 5720 | 33.36 | 9.12 | 50.23 | 40.65 | 71.19 | 11.56 | 0.76 | 0.44 | 16.06 |
| MBT | 6746 | 10.79 | 6.19 | 39.07 | 54.75 | 80.75 | 6.66 | 1.58 | 0.38 | 10.64 |
| WH | 6621 | 36.38 | 1.46 | 51.63 | 46.90 | 74.13 | 11.92 | 0.69 | 0.14 | 13.13 |
| WHT | 7055 | 15.59 | 4.44 | 41.95 | 53.61 | 82.33 | 7.45 | 1.61 | 0.25 | 8.36 |

**Table 2**
Fuel ratio and ignitability index of the raw and treated coals.

| Sample mark | Fuel ratio | Ii | Sample mark | Fuel ratio | Ii |
|---|---|---|---|---|---|
| ME | 0.80 | 31.30 | AR | 0.94 | 48.48 |
| MET | 0.99 | 64.74 | ART | 1.24 | 68.71 |
| TB | 0.90 | 30.11 | BP | 0.82 | 30.96 |
| TBT | 1.30 | 50.59 | BPT | 1.27 | 58.15 |
| BL | 0.81 | 31.78 | BJ | 0.76 | 34.96 |
| BLT | 1.04 | 70.16 | BJT | 1.38 | 62.58 |
| GM | 0.96 | 27.65 | BS | 0.89 | 40.61 |
| GMT | 1.11 | 55.79 | BST | 1.25 | 66.43 |
| KB | 0.93 | 33.86 | PP | 0.72 | 27.98 |
| KBT | 1.25 | 57.11 | PPT | 1.13 | 63.87 |
| TS | 0.85 | 22.51 | GB | 0.73 | 30.32 |
| TST | 1.39 | 55.14 | GBT | 0.90 | 60.54 |
| AD | 0.84 | 43.68 | MB | 0.81 | 24.21 |
| ADT | 0.98 | 67.75 | MBT | 1.40 | 45.18 |
| AK | 0.87 | 31.24 | WH | 0.91 | 25.93 |
| AKT | 1.24 | 52.04 | WHT | 1.28 | 44.90 |

considered a coalification process, although it occurs due to an increase in temperature and pressure [44].

After HTD, the nitrogen content in the treated coal samples increased slightly because of the reduced coal mass caused by moisture removal. The sulfur contents exhibited fluctuations, with certain instances of increase and others of decrease. The presence of various sulfur forms in the coal is likely the contributing factor. However, the increase in the nitrogen and/or sulfur contents did not significantly affect the NOx and SOx emissions when the coal was burned in the CFPPs because they were below the permissible threshold [45].

### 3.2. Effect of the HTD process on ash deposition

To study the effect of HTD on ash deposition, the chemical ash composition and AFT were investigated. The results of the ash composition analysis, where each oxide is represented as a mass fraction of the ash (wt%), are listed in Table 3. The indices used to predict the ash deposition of the raw and treated coal samples are listed in Table 4. The indices of the treated coal samples exhibited an increase in comparison to the raw coal samples, whereas certain indices demonstrated a decrease, contingent upon their ash chemical composition.

The AFT results for the raw and treated coal samples are listed in Table 5. The AFT characteristics under oxidative conditions were better than those under reductive conditions. The application of oxidative HTD circumstances resulted in a rise in all the AFTs. Conversely, the implementation of reductive conditions led to a mixed response among the AFTs, with some exhibiting an increase and others experiencing a decrease, attributable to the HTD process. A low AFT not only causes problems in removing liquid slag from the gasifier but also exacerbates fouling and slag formation on the heating surfaces of both the gasifier and combustion boiler, thereby limiting the overall process [46].

The AFT is essentially dependent on the chemical composition of coal ash. Generally, coal with a high $SiO_2$ content has a high AFT [47]. A high iron content in coal ash promotes liquid formation and the conversion of $Fe^{3+}$ to $Fe^{2+}$. Moreover, the presence of $Fe_2O_3$ in coal ash affects the fusibility under different conditions. Therefore, the AFT decreases with increasing iron content [48]. Most of the iron is in the $Fe^{2+}$ state and acts as a basic oxide to reduce the AFT [49]. The relationship between the ash composition of the

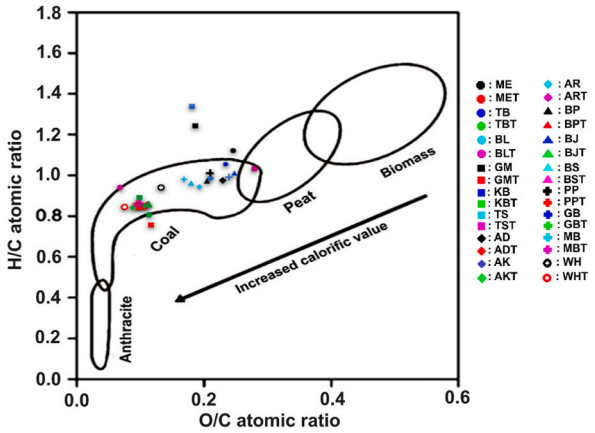


**Fig. 1.** Van Krevelen diagram of the raw and treated coals.

**Table 3**
Ash composition of the raw and treated coals (weight %).

| | $SiO_2$ | $Al_2O_3$ | $Fe_2O_3$ | $K_2O$ | $Na_2O$ | CaO | MgO | $TiO_2$ | MnO | $P_2O_5$ | $SO_3$ |
|---|---|---|---|---|---|---|---|---|---|---|---|
| ME | 31.5 | 18.29 | 19.96 | 0.6 | 1.66 | 12.43 | 5.03 | 0.89 | 1.2 | 0.1 | 7.41 |
| MET | 25.5 | 19.29 | 28.9 | 0.46 | 1.06 | 11.47 | 3.98 | 0.79 | 1.18 | 0.01 | 1.58 |
| TB | 39.7 | 24.0 | 16.97 | 1.12 | 0.42 | 6.11 | 2.33 | 1.13 | 0.13 | 0.22 | 6.25 |
| TBT | 40.9 | 28.0 | 17.6 | 0.65 | 0.23 | 5.74 | 1.38 | 1.1 | 0.15 | 0.6 | 2.06 |
| BL | 24.2 | 12.12 | 40.6 | 0.28 | 2.05 | 5.88 | 2.97 | 0.73 | 0.14 | nd | 7.7 |
| BLT | 24.8 | 8.96 | 54.5 | 0.1 | 0.15 | 2.26 | 1.77 | 0.7 | 0.48 | nd | 3.05 |
| GM | 24.6 | 5.89 | 0.52 | 0.61 | 3.01 | 1.59 | 7.13 | 44.9 | 0.10 | 1.47 | 9.01 |
| GMT | 19.2 | 6.61 | 0.23 | 0.06 | 1.82 | 0.3 | 3.49 | 63.8 | nd | 0.3 | 2.9 |
| KB | 24.5 | 53.4 | 8.82 | 0.78 | 0.091 | 4.64 | 2.18 | 2.31 | 0.12 | 0.18 | 1.1 |
| KBT | 12.85 | 40.2 | 31.2 | 0.28 | 0.27 | 3.54 | 1.18 | 2.21 | 0.19 | 0.05 | 3.86 |
| TS | 24.4 | 27.3 | 28 | 0.6 | 0.17 | 5.73 | 2.6 | 0.41 | 0.17 | 0.88 | 7.05 |
| TST | 21.9 | 22.6 | 45.2 | 0.37 | 0.26 | 2.35 | 1.41 | 0.33 | 0.26 | nd | 1.16 |
| AD | 38.1 | 7.29 | 26 | 0.27 | 0.19 | 11.1 | 7.76 | 0.77 | 0.58 | 0.05 | 7.13 |
| ADT | 23.3 | 6.62 | 48.5 | 0.64 | 1.56 | 6.19 | 5.92 | 0.63 | 0.56 | 0.06 | 5.04 |
| AK | 2.95 | 14.72 | 38.9 | 0.19 | 0.1 | 14.87 | 6.19 | 0.1 | 1.52 | 0.01 | 5.37 |
| AKT | 2.15 | 10.99 | 59.3 | 0.62 | 1.57 | 9.3 | 4.93 | 0.89 | 1.42 | 0.07 | 8.44 |
| AR | 26.6 | 6.28 | 19.96 | 0.64 | 0.67 | 21.2 | 9.62 | 0.38 | 0.21 | 0.05 | 12.4 |
| ART | 11.76 | 4.6 | 61.6 | 0.1 | 0.1 | 8.82 | 3.06 | 0.05 | 0.35 | 0.01 | 4.34 |
| BP | 3.35 | 8.5 | 62.9 | 0.19 | 0.11 | 10.03 | 3.05 | 0.07 | 1.39 | nd | 7.82 |
| BPT | 1.12 | 5.75 | 77.8 | 0.61 | 1.54 | 4.47 | 1.91 | 0.48 | 1.03 | 0.08 | 4.99 |
| BJ | 37.8 | 20.1 | 30.9 | 0.25 | 0.12 | 0.91 | 0.65 | 1.61 | 0.31 | 0.1 | 3.05 |
| BJT | 39.9 | 20 | 32.8 | 0.31 | 0.18 | 1.23 | 0.15 | 1.7 | 0.25 | 0.02 | 1.85 |
| BS | 44 | 17.26 | 15.97 | 0.53 | 1.09 | 7.43 | 4.06 | 0.41 | 0.07 | 0.07 | 5.89 |
| BST | 40.4 | 16.7 | 24.8 | 0.13 | 0.2 | 6.68 | 2.5 | 0.39 | 0.12 | 0.02 | 6.71 |
| PP | 14.6 | 5.9 | 22 | 0.83 | 0.35 | 19.21 | 3.59 | 0.31 | 0.19 | 0.12 | 32.3 |
| PPT | 11.6 | 7.31 | 34.56 | 0.66 | 0.64 | 20.9 | 3.09 | 0.31 | 0.27 | nd | 0.43 |
| GB | 4.1 | 0.58 | 89.8 | 0.03 | 0.043 | 1.32 | 0.14 | 0.77 | 1.77 | 0.2 | 0.99 |
| GBT | 1.21 | 1.3 | 91.3 | 0.24 | 0.53 | 1.42 | 0.3 | 0.26 | 1.49 | 0.14 | 0.43 |
| MB | 40.8 | 23.6 | 22 | 0.77 | 0.79 | 3.74 | 2.38 | 1.72 | 0.33 | 2.58 | 0.42 |
| MBT | 24.9 | 40.8 | 20.6 | 0.17 | 0.88 | 2.24 | 0.57 | 2.45 | 0.15 | nd | 2.62 |
| WH | 23.9 | 17.89 | 21.6 | 0.27 | 0.15 | 12.52 | 5.85 | 0.86 | 0.36 | 0.38 | 0.82 |
| WHT | 11.1 | 14.02 | 53.1 | 0.17 | 0.29 | 6.15 | 1.67 | 0.81 | 0.48 | nd | 1.96 |

Note.
nd: not detected.

normalized basic oxides, $Al_2O_3$, and $SiO_2$, and the AFT before and after oxidative HTD is shown in the pseudo-ternary diagram in Fig. 2. Acidic oxides, such as $SiO_2$, $Al_2O_3$, and $TiO_2$, increased the AFT by forming high-melting-point minerals. In contrast, basic oxides, such as CaO, MgO, $Na_2O$, and $K_2O$, decreased the AFT by generating low-melting-point minerals.

The vertical axis in Fig. 2 represents the AFT values (°C). The highest AFT is marked in gray, whereas the lowest is marked in blue. Generally, the AFT values are high for high levels of $SiO_2$ and $Al_2O_3$ and low levels of the basic oxides in terms of the mass ratio. Fig. 2 shows that the HTD process increased the AFT values under oxidative conditions. For the IDT, before the HTD process, the red area was relatively small; after HTD, it became larger, indicating that the AFT increased. The ST, HT, and FT AFTs before the HTD process are red, whereas after HTD they are gray. The increase in AFT after HTD may be due to the increased acidic oxide content, which easily combines with oxygen and is prone to forming polymer structures, thereby increasing the AFTs [28]. From this perspective, increasing the AFT value under oxidative conditions using the HTD process will reduce ash deposition.

However, it is challenging to determine whether the HTD process affects ash deposition during coal combustion in boilers or gasifiers based solely on the chemical ash composition and AFT. Therefore, statistical evaluation data were used to obtain the most influential parameters. It was assumed that 36 elements would influence ash deposition, including coal ash composition (% dry) and sulfur (% daf) (Table 2); the ash chemical composition (Table 4); the indices of ash deposition based on the ash chemical composition (Table 5); the AFTs (Table 6); and some additional variables [30], to complete the calculations listed in Table 6.

To determine the difference in ash deposition before and after the HTD process, Eqs. (13) and (14) were applied.

$$t_{count} = \frac{\underline{\delta}}{S_d/\sqrt{n}} \tag{13}$$

$$S_d = \sqrt{\frac{\sum \delta^2 - (\sum \delta)^2}{n-1}} \tag{14}$$

Where:

$\underline{\delta}$: the difference between the two averages of the paired data;

$S_d$: the standard deviation of the difference between the paired data;

n: the number of observations for the paired data.

**Table 4**
Some indices to predict the ash deposition.

| | B/A | BAI | Fu | SR | Rs |
|---|---|---|---|---|---|
| ME | 0.78 | 8.83 | 1.77 | 45.71 | 0.20 |
| MET | 1.01 | 19.01 | 1.53 | 36.51 | 0.19 |
| TB | 0.42 | 11.02 | 0.64 | 60.97 | 0.27 |
| TBT | 0.37 | 20.00 | 0.32 | 62.33 | 0.22 |
| BL | 1.40 | 17.42 | 3.26 | 32.86 | 4.26 |
| BLT | 1.71 | 218.00 | 0.43 | 29.76 | 5.49 |
| GM | 0.17 | 0.14 | 0.62 | 72.70 | 0.02 |
| GMT | 0.07 | 0.12 | 0.12 | 82.69 | 0.01 |
| KB | 0.21 | 10.13 | 0.18 | 61.04 | 0.04 |
| KBT | 0.66 | 56.73 | 0.36 | 26.35 | 0.14 |
| TS | 0.71 | 36.36 | 0.55 | 40.18 | 0.51 |
| TST | 1.11 | 71.75 | 0.70 | 30.91 | 0.66 |
| AD | 0.98 | 56.52 | 0.45 | 45.93 | 0.11 |
| ADT | 2.06 | 22.05 | 4.52 | 27.77 | 0.36 |
| AK | 3.39 | 134.14 | 0.98 | 4.69 | 0.61 |
| AKT | 5.40 | 27.08 | 11.82 | 2.84 | 1.21 |
| AR | 1.57 | 15.24 | 2.05 | 34.38 | 0.31 |
| ART | 4.49 | 308.00 | 0.90 | 13.80 | 0.51 |
| BP | 6.40 | 209.67 | 1.92 | 4.22 | 0.92 |
| BPT | 11.75 | 36.19 | 25.25 | 1.31 | 2.60 |
| BJ | 0.55 | 83.51 | 0.20 | 53.80 | 0.21 |
| BJT | 0.56 | 66.94 | 0.28 | 53.86 | 0.21 |
| BS | 0.47 | 9.86 | 0.76 | 61.57 | 1.00 |
| BST | 0.60 | 75.15 | 0.20 | 54.32 | 1.14 |
| PP | 2.21 | 18.64 | 2.61 | 24.58 | 4.46 |
| PPT | 3.11 | 26.58 | 4.05 | 16.54 | 5.64 |
| GB | 16.76 | 1197.3 | 1.26 | 4.30 | 2.68 |
| GBT | 33.86 | 118.57 | 26.07 | 1.28 | 2.82 |
| MB | 0.45 | 14.10 | 0.70 | 59.20 | 0.20 |
| MBT | 0.36 | 19.62 | 0.38 | 51.54 | 0.14 |
| WH | 0.95 | 51.43 | 0.40 | 37.42 | 0.09 |
| WHT | 2.37 | 115.43 | 1.09 | 15.41 | 0.50 |

The hypothesis is as follows:

$H_0$: μi = μj, there is no difference in the analysis results before and after the HTD process.

A: μi ≠ μj, there is a difference in the analysis results before and after the HTD process.

For example, one of the elements to be tested is the coal ash composition (% dry) before and after HTD, and thus the hypothesis is expressed as follows.

H: $\mu_i = \mu_j$, no difference in the coal ash content (% dry) before and after the HTD process.

A: $\mu_i \neq \mu_j$, a difference in the coal ash content (% dry) before and after the HTD process.

$$\overline{d} = \overline{X}_1 - \overline{X}_2 = 5.26 - 6.78 = -1.51$$

$$S_d = \sqrt{\frac{\sum d^2 - (\sum d)^2}{n-1}} = \sqrt{\frac{69.69 - (24.24)^2}{15}} = 0.3702$$

$$t_{count} = \frac{-1.51}{0.3702/\sqrt{16}} = -4.0954$$

From the calculations, Sd was 0.3702 and $t_{count} = |-4.0954| = 4.0954 > t_{table} = t(\alpha = 5\,\%/2, df = 15) = |-2.13| = 2.13$, and thus $H_0$ is rejected. Therefore, at a significance level of 5 %, there was a significant difference in ash content before and after HTD. The same method was used to calculate and test the remaining 35 variables. The calculation and testing of the two averages were performed using SPSS software. Based on the calculation results, 11 (eleven) variables significantly changed after the HTD process in terms of the coal ash composition (% dry), $SiO_2$, $Fe_2O_3$, CaO, MgO, SR, Rs, $IDT_{Ox}$, $ST_{Ox}$, $HT_{Ox,}$ and $FT_{Ox}$. In contrast, the other variables did not change significantly.

Therefore, these 11 variables are thought to significantly affect ash deposition during combustion due to the HTD process. By condensing these variables into factors using PCA, it is possible to simplify their identification and evaluation [38].

After the SPSS calculations, Bartlett's test of sphericity was performed, yielding a result of 211.051, with a significance level of 0.0001. This significance value is less than 0.05 (5 %), and the observational data were considered as samples that met the data adequacy requirements for analysis using PCA. The Kaiser–Meyer–Olkin measurement of sampling adequacy (KMO–MSA) value was 0.577, which is greater than 0.5 (Table 7, Step 1). This indicates that the datasets from the 11 variables could be processed. The next calculation (Step 2) was to test the MSA, namely, testing variables that can or cannot be processed or excluded from the dataset to be analyzed. In the preliminary analysis of the observed variables based on the MSA values, three variables, namely the ash composition,

**Table 5**
Ash fusion temperature of the raw and treated coals.

| Sample mark | Condition | IDT | ST | HT | FT | Sample mark | Condition | IDT | ST | HT | FT |
|---|---|---|---|---|---|---|---|---|---|---|---|
| ME | Reduction | 1110 | 1135 | 1150 | 1290 | AR | Reduction | 1235 | 1320 | 1330 | 1375 |
| | Oxidation | 1215 | 1255 | 1260 | 1345 | | Oxidation | 1290 | 1370 | 1375 | 1445 |
| MET | Reduction | 1100 | 1145 | 1160 | 1360 | ART | Reduction | 1300 | 1360 | 1375 | 1395 |
| | Oxidation | 1305 | 1365 | 1380 | 1460 | | Oxidation | 1375 | 1550 | 1550 | 1550 |
| TB | Reduction | 1235 | 1280 | 1290 | 1345 | BP | Reduction | 1225 | 1285 | 1310 | 1390 |
| | Oxidation | 1295 | 1330 | 1335 | 1355 | | Oxidation | 1550 | 1550 | 1550 | 1550 |
| TBT | Reduction | 1200 | 1240 | 1275 | 1400 | BPT | Reduction | 1265 | 1345 | 1355 | 1375 |
| | Oxidation | 1370 | 1430 | 1435 | 1445 | | Oxidation | 1550 | 1550 | 1550 | 1550 |
| BL | Reduction | 1120 | 1140 | 1165 | 1220 | BJ | Reduction | 1075 | 1190 | 1240 | 1330 |
| | Oxidation | 1320 | 1400 | 1430 | 1485 | | Oxidation | 1270 | 1350 | 1355 | 1400 |
| BLT | Reduction | 1055 | 1160 | 1175 | 1275 | BJT | Reduction | 1090 | 1170 | 1205 | 1355 |
| | Oxidation | 1365 | 1435 | 1450 | 1475 | | Oxidation | 1335 | 1350 | 1360 | 1380 |
| GM | Reduction | 1025 | 1110 | 1120 | 1275 | BS | Reduction | 1095 | 1175 | 1195 | 1315 |
| | Oxidation | 1280 | 1320 | 1350 | 1495 | | Oxidation | 1200 | 1260 | 1270 | 1330 |
| GMT | Reduction | 1125 | 1155 | 1165 | 1220 | BST | Reduction | 1075 | 1135 | 1175 | 1335 |
| | Oxidation | 1415 | 1475 | 1485 | 1550 | | Oxidation | 1230 | 1305 | 1320 | 1360 |
| KB | Reduction | 1345 | 1550 | 1550 | 1550 | PP | Reduction | 1255 | 1275 | 1285 | 1340 |
| | Oxidation | 1400 | 1550 | 1550 | 1550 | | Oxidation | 1290 | 1310 | 1315 | 1380 |
| KBT | Reduction | 1550 | 1550 | 1550 | 1550 | PPT | Reduction | 1150 | 1255 | 1260 | 1280 |
| | Oxidation | 1550 | 1550 | 1550 | 1550 | | Oxidation | 1310 | 1320 | 1330 | 1425 |
| TS | Reduction | 1245 | 1295 | 1335 | 1415 | GB | Reduction | 1285 | 1315 | 1325 | 1335 |
| | Oxidation | 1345 | 1383 | 1410 | 1460 | | Oxidation | 1485 | 1550 | 1550 | 1550 |
| TST | Reduction | 1195 | 1290 | 1320 | 1435 | GBT | Reduction | 1300 | 1335 | 1340 | 1345 |
| | Oxidation | 1380 | 1445 | 1465 | 1485 | | Oxidation | 1550 | 1550 | 1550 | 1550 |
| AD | Reduction | 1050 | 1110 | 1135 | 1210 | MB | Reduction | 1105 | 1170 | 1200 | 1335 |
| | Oxidation | 1155 | 1225 | 1230 | 1360 | | Oxidation | 1300 | 1345 | 1360 | 1405 |
| ADT | Reduction | 1120 | 1155 | 1160 | 1175 | MBT | Reduction | 1410 | 1550 | 1550 | 1550 |
| | Oxidation | 1310 | 1405 | 1425 | 1495 | | Oxidation | 1415 | 1550 | 1550 | 1550 |
| AK | Reduction | 1110 | 1210 | 1230 | 1290 | WH | Reduction | 1265 | 1340 | 1375 | 1550 |
| | Oxidation | 1375 | 1410 | 1465 | 1550 | | Oxidation | 1360 | 1445 | 1475 | 1550 |
| AKT | Reduction | 1235 | 1335 | 1355 | 1550 | WHT | Reduction | 1300 | 1375 | 1425 | 1550 |
| | Oxidation | 1440 | 1550 | 1550 | 1550 | | Oxidation | 1440 | 1550 | 1550 | 1550 |

CaO, and MgO, had values of less than 0.5. This implies that these variables did not meet the requirements for inclusion in the PCA; therefore, they were excluded. A recalculation was performed for the ash composition (% dry) variable, and the KMO–MSA value was 0.552, which is greater than 0.5, with a sphericity of 204.867 (Table 8, Step 2). Subsequent calculations involved only the remaining eight variables. The KMO–MSA values of the eight variables are 0.694 (>0.5), as listed in Table 7 (Step 3). Therefore, the datasets of the eight tested variables meet the MSA requirements and can be included in the PCA.

The number of components was determined using the Eigen values listed in Table 8, which was measured based on the percentage variance, with component 1 having a cumulative variance of 62.939 %, and component 2 having a cumulative variance of 86.430 %. This implied that the eight variables could be explained by the two identified components.

The extraction values indicated the reinforced communality value of each variable. The component matrix (two components) and the average values of the components of the raw and treated coal samples are listed in Table 9. The highest communality value is the $HT_{Ox}$ variable, which was 0.968 (97 %). This implies that this value is closely related to the contributing factors. The lowest communality value is the Rs variable, which was 0.723 (72 %). Generally, the eight variables can be explained by the factors included in the PCA.

Component 1 was closely correlated with the $Fe_2O_3$, Rs, $IDT_{Ox}$, $ST_{Ox}$, $HT_{Ox}$, and $FT_{Ox}$ variables. Ash deposition decreased by factors of 0.891 and 0.716 with an increase in $SiO_2$ and SR of one unit, respectively. Component 2 correlated only with the $SiO_2$ and SR variables, and ash deposition decreased by factors of 0.566 and 0.846, respectively, with an increase in $Fe_2O_3$, and Rs o one unit. In contrast, the $ST_{Ox}$ and $HT_{Ox}$ variables were affected the most by increases in ash deposition, with values of 0.914 and 0.913 for each unit increase, respectively. Therefore, $SiO_2$, $Fe_2O_3$, SR, Rs, $IDT_{Ox}$, $ST_{Ox}$, $HT_{OX}$, and $FT_{Ox}$ had dominant roles in the ash chemical composition and AFT during the HTD process.

Notably, a high SR index indicates a high slag viscosity, and thus low slagging. If the SR index is $> 72$, the tendency to form impurities is low. If the SR index ranges between 65 and 72, the tendency to form impurities is average, and if the SR index is $< 65$, the tendency to form impurities is very high [46]. The prediction of the slagging or Rs at the furnace wall during boiler operation was based on the B/A ratio of the coal ash and the percentage of sulfur in the coal sample on a dry basis.

$SiO_2$ and $FeO/Fe_2O_3$ are the main components of coal ash. The $SiO_2$ content of coal influenced the AFT. Coal with a high $SiO_2$ content had a low AFT. The $SiO_2$ content of the treated coal samples was generally lower than that of the raw coal samples. Meanwhile, the $Fe_2O_3$ content increased because of the HTD process. $Fe_2O_3$ was used as a flux agent, which more clearly reduced the AFTs [46]. The treated coal samples had a lower SR than the raw coal samples. Both had SR values of <65, and thus exhibited high ash deposition. The slagging index or Rs of the treated coal samples was higher than those of the raw coal samples. However, the average values of the raw and treated coals were within the same intermediate level of slagging (0.6–2.0) [29]. The AFTs of IDT, ST, HT, and FT of the

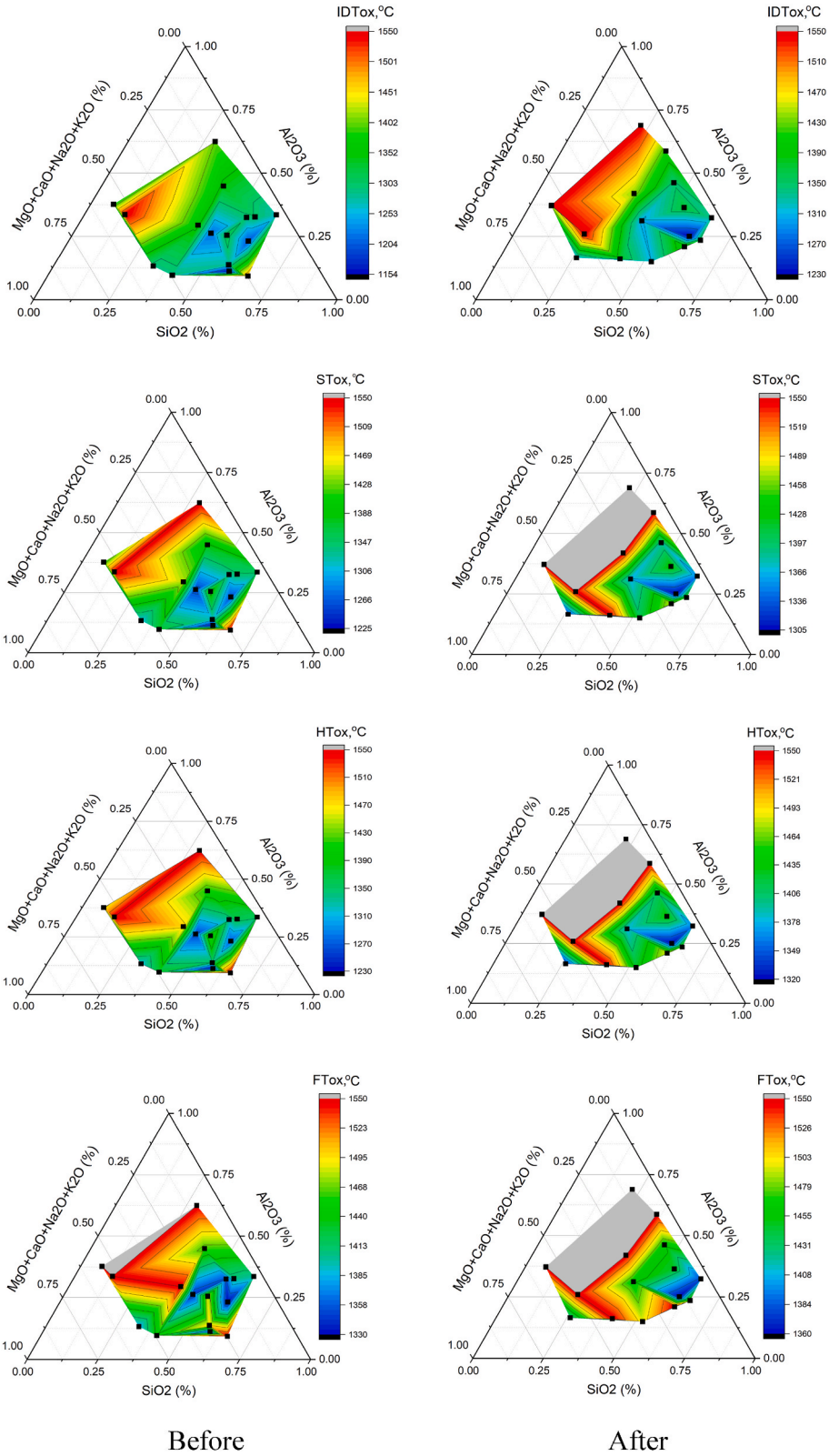


**Fig. 2.** Relationship between ash composition and AFT before and after oxidative HTD.

**Table 6**
Variables calculated based on ash chemical composition analysis.

| | Si/(Ca + Mg) | (Si + P + K)/(Ca + Mg) | Si/K | Al/200 | Fe/Mn | B/A + P |
|---|---|---|---|---|---|---|
| ME | 1.80 | 1.84 | 52.50 | 0.09 | 16.63 | 0.88 |
| MET | 1.65 | 1.68 | 55.43 | 0.10 | 24.49 | 1.01 |
| TB | 4.70 | 4.86 | 35.45 | 0.12 | 130.54 | 0.64 |
| TBT | 5.74 | 5.92 | 62.92 | 0.14 | 117.33 | 0.97 |
| BL | 2.73 | – | 86.43 | 0.06 | 290.00 | – |
| BLT | 6.15 | – | 248.00 | 0.04 | 113.54 | – |
| GM | 2.82 | 3.06 | 40.33 | 0.03 | 5.31 | 1.64 |
| GMT | 5.07 | 5.16 | 304.76 | 0.03 | – | 0.37 |
| KB | 3.59 | 3.73 | 31.41 | 0.27 | 73.50 | 0.39 |
| KBT | 2.72 | 2.79 | 45.89 | 0.20 | 164.21 | 0.71 |
| TS | 2.93 | 3.11 | 40.67 | 0.14 | 164.71 | 1.59 |
| TST | 5.82 | – | 59.19 | 0.11 | 173.85 | – |
| AD | 2.02 | 2.04 | 141.11 | 0.04 | 44.83 | 1.04 |
| ADT | 1.92 | 1.98 | 36.41 | 0.03 | 86.61 | 2.12 |
| AK | 0.14 | 0.15 | 15.53 | 0.07 | 25.59 | 3.39 |
| AKT | 0.15 | 0.20 | 3.47 | 0.05 | 41.76 | 5.47 |
| AR | 0.86 | 0.89 | 41.56 | 0.03 | 95.05 | 1.62 |
| ART | 0.99 | 1.00 | 117.60 | 0.02 | 176.00 | 4.49 |
| BP | 0.26 | – | 17.63 | 0.04 | 45.25 | – |
| BPT | 0.18 | 0.28 | 1.84 | 0.03 | 75.53 | 11.83 |
| BJ | 24.23 | 24.46 | 151.20 | 0.10 | 99.68 | 0.65 |
| BJT | 28.91 | 29.15 | 128.71 | 0.10 | 131.20 | 0.58 |
| BS | 3.83 | 3.88 | 83.02 | 0.09 | 228.14 | 0.55 |
| BST | 4.40 | 4.42 | 310.77 | 0.08 | 206.67 | 0.62 |
| PP | 0.64 | 0.68 | 17.59 | 0.03 | 115.79 | 2.33 |
| PPT | 0.48 | – | 17.58 | 0.04 | 128.00 | – |
| GB | 2.81 | 2.97 | 128.13 | 0.00 | 50.73 | 16.96 |
| GBT | 0.70 | 0.92 | 5.04 | 0.01 | 61.28 | 34.00 |
| MB | 6.67 | 7.21 | 52.99 | 0.12 | 66.67 | 3.03 |
| MBT | 8.86 | – | 146.47 | 0.20 | 137.33 | – |
| WH | 1.30 | 1.34 | 88.52 | 0.09 | 60.00 | 1.33 |
| WHT | 1.42 | – | 65.29 | 0.07 | 110.63 | – |

**Table 7**
KMO and Bartlett's test.

| KMO-MSA | | Step 1 | Step 2 | Step 3 |
|---|---|---|---|---|
| | | 0.577 | 0.552 | 0.694 |
| Bartlett's Test of Sphericity | Approx. Chi-Square | 211.051 | 204.867 | 170.605 |
| | df | 0.55 | 45 | 28 |
| | Sig. | 0 | 0 | 0 |

**Table 8**
Total variance explained[a].

| Component | Initial Eigenvalues | | | Extraction Sums of Squared Loadings | | | Rotation Sums of Squared Loadings | | |
|---|---|---|---|---|---|---|---|---|---|
| | Total | Variance % | Cumulative % | Total | Variance % | Cumulative % | Total | Variance % | Cumulative % |
| 1 | 5.035 | 62.939 | 62.939 | 5.035 | 62.939 | 62.939 | 4.358 | 54.478 | 54.478 |
| 2 | 1.879 | 23.492 | 86.430 | 1.879 | 23.492 | 86.430 | 2.556 | 31.952 | 86.430 |
| 3 | 0.512 | 6.402 | 92.833 | | | | | | |
| 4 | 0.285 | 3.566 | 96.398 | | | | | | |
| 5 | 0.194 | 2.421 | 98.820 | | | | | | |
| 6 | 0.071 | 0.890 | 99.710 | | | | | | |
| 7 | 0.022 | 0.280 | 99.989 | | | | | | |
| 8 | 0.001 | 0.011 | 100.000 | | | | | | |

[a] Extraction Method: PCA.

treated coal samples under oxidative conditions were higher than those of the raw coal samples, and it could be burned at a temperature of >1400 °C. These results are consistent with those reported by Yang et al. [20].

Based on the average values of these parameters and the ash chemical analysis results, the treated and raw coal samples have a similar ash deposition tendency. Based on the AFT under oxidative conditions, the treated coal samples had a higher AFT value,

**Table 9**
Extraction value*, Component Matrix (two components extracted), and average values of the raw and treated coals.

| Element | Initial | Extraction | Component | | Raw | Treated |
|---|---|---|---|---|---|---|
| | | | 1 | 2 | | |
| $SiO_2$ | 1 | 0.858 | −0.891 | 0.254 | 25.32 | 19.54 |
| $Fe_2O_3$ | 1 | 0.815 | 0.703 | −0.566 | 29.06 | 42.62 |
| SR | 1 | 0.876 | −0.716 | 0.603 | 40.22 | 31.7 |
| Rs | 1 | 0.723 | 0.083 | −0.846 | 1.12 | 1.47 |
| $IDT_{Ox}$ | 1 | 0.793 | 0.872 | 0.177 | 1321 | 1394 |
| $ST_{Ox}$ | 1 | 0.966 | 0.914 | 0.361 | 1378 | 1457 |
| $HT_{Ox}$ | 1 | 0.968 | 0.913 | 0.366 | 1393 | 1465 |
| $FT_{Ox}$ | 1 | 0.915 | 0.893 | 0.344 | 1451 | 1494 |

a Extraction Method: PCA.

indicating that its tendency for ash deposition was lower. This implies that the HTD process can improve the quality of low-grade coal.

To date, research on the factors affecting ash deposition during the HTD process has not been conducted. Some researchers have reported that HTD improves the quality of coal by enhancing the combustion characteristics and lowering the tendency for slagging and fouling compared to raw coal [5,8,9,18]. Yang et al. reported that after the HTD process, $SiO_2$ increased and $Fe_2O_3$ decreased [20]. Moreover, Wan et al. reported that $Fe_2O_3$ decreased after HTD [19]. In this study, the opposite trend was observed; generally, $SiO_2$ decreased and $Fe_2O_3$ increased. This is most likely due to the differences in the type of coal used, because coal is a heterogeneous mixture of organic and inorganic matter. Coal ash deposition is influenced by the type of mineral present in coal [50]. A significant amount of silica indicates the presence of clay minerals such as shale, slate, and silicates in the coal [51]. A high $Fe_2O_3$ content indicates the presence of inorganic species, which are associated with sulfur in the mineral pyrite and jarosite. However, iron also occurs as a trace element in kaolinite, which is a major clay mineral in coal [52].

The propensity for deposition, fouling, and slagging depends on the thermodynamics and kinetics of the mineral transformation [53]. Several drawbacks of the AFT method for studying ash fusion behavior have been reported by Yan et al. [54]. Among them are IDT variations for the same sample reported by different laboratories, which reached temperatures of 400 °C. Therefore, AFT cannot quantitatively represent the entire fusion process. To improve the repeatability and reproducibility of the ash fusibility test, thermomechanical analysis (TMA) should be conducted in the near future. This method directly measures the ash fusion behavior based on its mechanical characteristics [55]. Moreover, it may provide a better understanding of the entire fusion process and facilitate the elucidation of the ash deposition and sintering mechanisms.

## 4. Conclusion

The HTD process improved the quality of low-grade coal to equal that of high-grade coal. The moisture content of the coal decreased significantly, and the calorific value, fuel ratio, and ignitability index of the treated coal samples were higher than those of the raw coal samples. It was difficult to determine the effect of the HTD process on ash deposition by relying only on the results of the ash chemical composition variables. Therefore, in this study, statistical tests were conducted to determine the dominant parameters influencing ash deposition during the HTD process. The paired sample *t*-test and PCA methods were conducted using the SPSS software, and of the 36 variable parameters investigated, eight were determined to be the most influential factors for ash deposition due to the HTD process: $SiO_2$, $Fe_2O_3$, SR, Rs, $IDT_{Ox}$, $ST_{Ox}$, HTOx, and $FT_{Ox}$. To further investigate the effect of HTD on ash deposition, TMA will be conducted in the near future, where its success will contribute to minimizing ash disturbance in coal combustion as a transition energy towards green energy in Indonesia.

## 5. Data availability statement

All data generated in this study are included in the article.

## Additional information

No additional information is available for this paper.

## CRediT authorship contribution statement

**Datin Fatia Umar:** Writing – review & editing, Writing – original draft, Validation, Resources, Methodology, Investigation, Formal analysis, Data curation, Conceptualization. **Zulfahmi Zulfahmi:** Writing – review & editing, Writing – original draft, Validation, Software, Methodology, Investigation, Formal analysis, Data curation. **Triswan Suseno:** Writing – review & editing, Writing – original draft, Software, Methodology, Formal analysis, Data curation. **Suganal Suganal:** Writing – review & editing, Writing – original draft, Resources, Methodology, Formal analysis, Data curation. **Nendaryono Madiutomo:** Writing – review & editing, Methodology, Formal analysis, Data curation. **Liston Setiawan:** Writing – review & editing, Validation, Methodology, Investigation, Data curation. **Edwin Akhdiat Daranin:** Writing – original draft, Software, Investigation, Formal analysis, Data curation. **Gunawan Gunawan:** Writing –

review & editing, Validation, Software, Investigation, Formal analysis.

## Declaration of competing interest

The authors declare the following financial interests/personal relationships which may be considered as potential competing interests:Datin Fatia Umar reports were provided by the National Research and Innovation Agency Republic of Indonesia. Datin Fatia Umar reports a relationship with the National Research and Innovation Agency Republic of Indonesia that includes: employment. Authors previously employed by the Ministry of Energy and Mineral Resources, the Republic of Indonesia If there are other authors, they declare that they have no known competing financial interests or personal relationships that could have appeared to influence the work reported in this paper.

## Acknowledgements

The authors gratefully acknowledge the Head of Mining Technology Research Centre, BRIN, the Head of Geological Resources Research Centre, BRIN, Dr. Sihyun Lee, Dr. Jihoo Yo, and Mr. Wijaya Bangun Adi from the Korea Institute of Energy Research (KIER) for the valuable discussion and recommendation, the coal laboratory staff of the Mineral and Coal Testing Centre, the Ministry of Energy and Mineral Resources (MEMR), and all colleagues involved in this activity.

## References

[1] S.A. Wibisono, E.P. Dwitama, I.O. Prahesti, "Petrography and coal Geochemistry in Pahirangan and surrounding area, Kotawaringin Timur District, Central Kalimantan Province, Geological Resources Bulletin 14 (1) (May 2019) 65–78, https://doi.org/10.47599/bsdg.v14i1.245. In Indonesian),".
[2] A. Juarsa, S.A. Wibisono, M. Ibrahim, P. Oktaviani, R. Hidayat, Fatimah, Coal resources, in: Indonesia Mineral, Coal and Geothermal Resources and Reserves Balance Sheet 2021, Bandung: Centre of Mineral, Coal and Geothermal Resources Geological Agency, MEMR, 2022, pp. 94–114.
[3] M. Rahman, D. Pudasainee, R. Gupta, Review on chemical upgrading of coal: Production processes, potential applications and recent developments, Fuel Process. Technol. 158 (Apr. 2017) 35–56, https://doi.org/10.1016/j.fuproc.2016.12.010.
[4] Z. Rao, Y. Zhao, C. Huang, C. Duan, J. He, Recent developments in drying and dewatering for low rank coals, Prog. Energy Combust. Sci. 46 (Feb. 2015) 1–11, https://doi.org/10.1016/j.pecs.2014.09.001.
[5] C. Zhu, H. Tu, Y. Bai, D. Ma, Y. Zhao, Evaluation of slagging and fouling characteristics during Zhundong coal co-firing with a Si/Al dominated low rank coal, Fuel 254 (Oct. 2019), 115730, https://doi.org/10.1016/j.fuel.2019.115730.
[6] G. Favas, Hydrothermal dewatering of lower rank coals. 2. Effects of coal characteristics for a range of Australian and international coals, Fuel 82 (1) (Jan. 2003) 59–69, https://doi.org/10.1016/S0016-2361(02)00191-6.
[7] J. Wu, J. Liu, X. Zhang, Z. Wang, J. Zhou, K. Cen, Chemical and structural changes in XiMeng lignite and its carbon migration during hydrothermal dewatering, Fuel 148 (May 2015) 139–144, https://doi.org/10.1016/j.fuel.2015.01.102.
[8] L. Ge, Y. Zhang, C. Xu, Z. Wang, J. Zhou, K. Cen, Influence of the hydrothermal dewatering on the combustion characteristics of Chinese low-rank coals, Appl. Therm. Eng. 90 (Nov. 2015) 174–181, https://doi.org/10.1016/j.applthermaleng.2015.07.015.
[9] J. Liao, Y. Fei, M. Marshall, A.L. Chaffee, L. Chang, Hydrothermal dewatering of a Chinese lignite and properties of the solid products, Fuel 180 (Sep. 2016) 473–480, https://doi.org/10.1016/j.fuel.2016.04.027.
[10] A.P. Afin, B. Kiono, Coal energy potential; utilization and technology in Indonesia in 2020 – 2050: coal gasification (in Indonesian)_, New and Renewabale Journal 2 (2) (2021) 114–122.
[11] I. Panagiotidis, K. Vafiadis, A. Tourlidakis, A. Tomboulides, Study of slagging and fouling mechanisms in a lignite-fired power plant, Appl. Therm. Eng. 74 (Jan. 2015) 156–164, https://doi.org/10.1016/j.applthermaleng.2014.03.043.
[12] Y. Niu, Y. Zhu, H. Tan, S. Hui, Z. Jing, W. Xu, Investigations on biomass slagging in utility boiler: Criterion numbers and slagging growth mechanisms, Fuel Process. Technol. 128 (Dec. 2014) 499–508, https://doi.org/10.1016/j.fuproc.2014.07.038.
[13] K.M. Zierold, C. Odoh, A review on fly ash from coal-fired power plants: chemical composition, regulations, and health evidence, Rev. Environ. Health 35 (4) (Nov. 2020) 401–418, https://doi.org/10.1515/reveh-2019-0039.
[14] S. Samsudin, N.A. Aziz, A.A. Hairuddin, S.U. Masuri, A study on bituminous coal base acid ratio to the slagging factor at large scale boiler, International Journal of Heat and Technology 39 (3) (Jun. 2021) 833–840, https://doi.org/10.18280/ijht.390317.
[15] A. Trivedi, V.K. Sud, Collapse behavior of coal ash, J. Geotech. Geoenviron. Eng. 130 (4) (Apr. 2004) 403–415, https://doi.org/10.1061/(ASCE)1090-0241(2004)130:4(403).
[16] F. Frandsen, Empirical Prediction of Ash Deposition Propensities in Coal-Fired Utilities, Jan. 1997.
[17] A. Lawrence, R. Kumar, K. Nandakumar, K. Narayanan, A Novel tool for assessing slagging propensity of coals in PF boilers, Fuel 87 (6) (May 2008) 946–950, https://doi.org/10.1016/j.fuel.2007.07.028.
[18] Y. Zhang, et al., Effect of hydrothermal dewatering on the physico-chemical structure and surface properties of Shengli lignite, Fuel 164 (Jan. 2016) 128–133, https://doi.org/10.1016/j.fuel.2015.09.055.
[19] K. Wan, D. Pudasainee, V. Kurian, Z. Miao, R. Gupta, Changes in Physicochemical properties and the release of inorganic species during hydrothermal dewatering of lignite, Ind. Eng. Chem. Res. 58 (29) (Jul. 2019) 13294–13302, https://doi.org/10.1021/acs.iecr.9b01691.
[20] M. Yang, Q. Xie, X. Wang, H. Dong, H. Zhang, C. Li, Lowering ash slagging and fouling tendency of high-alkali coal by hydrothermal pretreatment, Int. J. Min. Sci. Technol. 29 (3) (May 2019) 521–525, https://doi.org/10.1016/j.ijmst.2018.05.007.
[21] T. Yan, J. Bai, L. Kong, Z. Bai, W. Li, J. Xu, Effect of SiO2/Al2O3on fusion behavior of coal ash at high temperature, Fuel 193 (2017) 275–283, https://doi.org/10.1016/j.fuel.2016.12.073.
[22] Haewon Kim, Chanseok Park, Min Wang, Paired t-test based on robustified statistics, in: Fall Conference, Korean Institute of Industrial Engineers, Seoul, Korea: Korean Institute of Industrial Engineers, Nov. 2018.
[23] T. Zeng, A. Mlonka-Mędrala, V. Lenz, M. Nelles, Evaluation of bottom ash slagging risk during combustion of herbaceous and woody biomass fuels in a small-scale boiler by principal component analysis, Biomass Convers Biorefin 11 (4) (Aug. 2021) 1211–1229, https://doi.org/10.1007/s13399-019-00494-2.
[24] D.F. Umar, I. Monika, S. Suganal, "Effect of hydrothermal processing of low rank coal on ash composition and melting point temperature, Journal of Mineral and Coal Technology 16 (3) (2020) in Indonesian),".
[25] M. Tongco, Purposive sampling as a tool for informant selection, Ethnobot. Res. Appl. 5 (2007) 147–158.
[26] M. Markič, Z. Kalan, J. Pezdič, J. Faganeli, H/C versus O/C atomic ratio characterization of selected coals in Slovenia, Geologija 50 (2) (Dec. 2007) 403–426, https://doi.org/10.5474/geologija.2007.028.
[27] D.F. Umar, M. Shimojo, R.M.N. Madiutomo, Evaluation of combustion behaviour for Indonesian low-rank coals treated hydrothermally, Indonesian Mining Journal 21 (2) (Oct. 2018) 127–139, https://doi.org/10.30556/imj.Vol21.No2.2018.919.

[28] J. Yu, X. Li, D. Fleming, Z. Meng, D. Wang, A. Tahmasebi, Analysis on characteristics of fly ash from coal fired power Stations, Energy Proc. 17 (2012) 3–9, https://doi.org/10.1016/j.egypro.2012.02.054.
[29] B. Kamara, D.V. Von Kallon, P.M. Mashinini, Fouling and slagging investigation on ash derived from Sasol coal using ICP and XRF Analytical techniques, Appl. Sci. 12 (22) (Nov. 2022), 11560, https://doi.org/10.3390/app122211560.
[30] T. Zeng, A. Mlonka-Mędrala, V. Lenz, M. Nelles, Evaluation of bottom ash slagging risk during combustion of herbaceous and woody biomass fuels in a small-scale boiler by principal component analysis, Biomass Convers Biorefin 11 (4) (Aug. 2021) 1211–1229, https://doi.org/10.1007/s13399-019-00494-2.
[31] Y. Lee, J. Kim, D. Kim, Y. Lee, Experimental study of Co-firing and emission characteristics fueled by Sewage Sludge and Wood Pellet in Bubbling fluidized bed, Clean Technology 23 (1) (Mar. 2017) 80–89, https://doi.org/10.7464/ksct.2017.23.1.080.
[32] F. Xiang, et al., Influence of hydrothermal dewatering on trace element transfer in Yimin coal, Appl. Therm. Eng. 117 (May 2017) 675–681, https://doi.org/10.1016/j.applthermaleng.2016.12.100.
[33] X. Yang, D. Ingham, L. Ma, N. Srinivasan, M. Pourkashanian, Ash deposition propensity of coals/blends combustion in boilers: a modeling analysis based on multi-slagging routes, Proc. Combust. Inst. 36 (3) (2017) 3341–3350, https://doi.org/10.1016/j.proci.2016.06.060.
[34] X.D. Chen, L.X. Kong, J. Bai, Z.Q. Bai, W. Li, Study on fusibility of coal ash rich in sodium and sulfur by synthetic ash under different atmospheres, Fuel 202 (2017) 175–183, https://doi.org/10.1016/j.fuel.2017.04.001.
[35] H. Li, et al., Effect of coal Blending on ash fusibility and Slurryability of Xinjiang low-rank coal, Processes 10 (9) (Aug. 2022) 1693, https://doi.org/10.3390/pr10091693.
[36] S.S. Tambe, M. Naniwadekar, S. Tiwary, A. Mukherjee, T.B. Das, Prediction of coal ash fusion temperatures using computational intelligence based models, Int J Coal Sci Technol 5 (4) (Dec. 2018) 486–507, https://doi.org/10.1007/s40789-018-0213-6.
[37] T. Yin, A. Othman, When does the pooled variance t-test fail, African J. Math. Comput. Sci. Res 2 (4) (2009) 56–62.
[38] S. Mishra, et al., Principal component analysis, International Journal of Livestock Research 1 (2017), https://doi.org/10.5455/ijlr.20170415115235.
[39] S. Aich, B.K. Nandi, S. Bhattacharya, Effect of weathering on physico-chemical properties and combustion behavior of an Indian thermal coal, Int J Coal Sci Technol 6 (1) (Mar. 2019) 51–62, https://doi.org/10.1007/s40789-018-0235-0.
[40] S. Aich, D. Behera, B.K. Nandi, S. Bhattacharya, Relationship between proximate analysis parameters and combustion behaviour of high ash Indian coal, Int J Coal Sci Technol 7 (4) (Dec. 2020) 766–777, https://doi.org/10.1007/s40789-020-00312-5.
[41] J. Faúndez, A. Arenillas, F. Rubiera, X. García, A.L. Gordon, J.J. Pis, Ignition behaviour of different rank coals in an entrained flow reactor, Fuel 84 (17) (Dec. 2005) 2172–2177, https://doi.org/10.1016/j.fuel.2005.03.028.
[42] A.A. Adeleke, J.K. Odusote, P.P. Ikubanni, O.A. Lasode, M. Malathi, D. Paswan, The ignitability, fuel ratio and ash fusion temperatures of torrefied woody biomass, Heliyon 6 (3) (Mar. 2020), e03582, https://doi.org/10.1016/j.heliyon.2020.e03582.
[43] P. Sethi, R.N. Mohapatro, R.S. Mohanty, S.K. Seet, R. Nagarajan, G.G. Roy, Study on spontaneous combustion of boiler Grade coal and Optimization of Consumption at Rinl, IOP Conf. Ser. Mater. Sci. Eng. 455 (Dec. 2018), 012086, https://doi.org/10.1088/1757-899X/455/1/012086.
[44] Y. Fei, et al., Comparison of some physico–chemical properties of Victorian lignite dewatered under non-evaporative conditions, Fuel 85 (14–15) (Oct. 2006) 1987–1991, https://doi.org/10.1016/j.fuel.2006.03.023.
[45] Anonym, Environmental Impact Analysis of Coal Power Generation Unit 4 Development Plan, 2015. Surabaya.
[46] A. Kowalczyk-Juśko, The influence of the ash from the biomass on the power boiler pollution, Journal of Ecological Engineering 18 (6) (Nov. 2017) 200–204, https://doi.org/10.12911/22998993/76897.
[47] Q.H. Li, Y.G. Zhang, A.H. Meng, L. Li, G.X. Li, Study on ash fusion temperature using original and simulated biomass ashes, Fuel Process. Technol. 107 (Mar. 2013) 107–112, https://doi.org/10.1016/j.fuproc.2012.08.012.
[48] C. He, et al., Effect of iron valence distribution on ash fusion behavior under Ar atmosphere by a metallic iron addition in the synthetic coal ash, Fuel 310 (Feb. 2022), 122340, https://doi.org/10.1016/j.fuel.2021.122340.
[49] Q. Wang, K. Han, J. Gao, J. Wang, C. Lu, Investigation of maize Straw char Briquette ash fusion characteristics and the influence of Phosphorus Additives, Energy Fuel. 31 (3) (Mar. 2017) 2822–2830, https://doi.org/10.1021/acs.energyfuels.7b00047.
[50] W.-J. Shi, et al., Effect of CaO/Fe2O3 on fusion behaviors of coal ash at high temperatures, Fuel Process. Technol. 181 (Dec. 2018) 18–24, https://doi.org/10.1016/j.fuproc.2018.09.007.
[51] S. Nasir, Demineralization of a low-rank coal to produce clean coal for Industrial utilization, Insights in Mining Science & Technology 2 (3) (Dec. 2020), https://doi.org/10.19080/IMST.2020.02.555590.
[52] F.B. Waanders, E. Vinken, A. Mans, A.F. Mulaba-Bafubiandi, Iron minerals in coal, Weathered coal and coal ash – SEM and Mössbauer results, Hyperfine Interact. 148/149 (2003) 21–29, https://doi.org/10.1023/B:HYPE.0000003760.89706.f6, no. 1–4.
[53] J. Tomeczek, H. Palugniok, Kinetics of mineral matter transformation during coal combustion, Fuel 81 (10) (Jul. 2002) 1251–1258, https://doi.org/10.1016/S0016-2361(02)00027-3.
[54] T. Yan, L. Kong, J. Bai, Z. Bai, W. Li, Thermomechanical analysis of coal ash fusion behavior, Chem. Eng. Sci. 147 (Jun. 2016) 74–82, https://doi.org/10.1016/j.ces.2016.03.016.
[55] Y. Liu, R. Gupta, L. Elliott, T. Wall, T. Fujimori, Thermomechanical analysis of laboratory ash, combustion ash and deposits from coal combustion, Fuel Process. Technol. 88 (11–12) (Dec. 2007) 1099–1107, https://doi.org/10.1016/j.fuproc.2007.06.028.